

Evidence for Electronic Phase Separation between Orbital Orderings in SmVO_3

M. H. Sage,¹ G. R. Blake,¹ G. J. Nieuwenhuys,² and T. T. M. Palstra^{1,*}

¹*Solid State Chemistry Laboratory, Materials Science Centre, University of Groningen, Nijenborgh 4, 9747 AG Groningen, The Netherlands*

²*Kamerlingh Onnes Laboratorium, Leiden University, P.O. Box 9504, 2300 RA Leiden, The Netherlands*
(Received 10 June 2005; published 23 January 2006)

We report evidence for phase coexistence of orbital orderings of different symmetry in SmVO_3 by high resolution x-ray powder diffraction. The phase coexistence is triggered by an antiferromagnetic ordering of the vanadium spins near 130 K, below an initial orbital ordering near 200 K. The phase coexistence is the result of the intermediate ionic size of samarium coupled to exchange striction at the vanadium spin ordering.

DOI: [10.1103/PhysRevLett.96.036401](https://doi.org/10.1103/PhysRevLett.96.036401)

PACS numbers: 71.70.Ej, 61.10.Nz, 61.50.Ks

In recent years, it has been shown that transition metal oxides with competing interactions involving spin, charge, and orbital degrees of freedom can exhibit a coexistence of different electronic phases, often associated with a coupling of the electronic degrees of freedom to the lattice. Much interest has been triggered by colossal magnetoresistance materials where a metal-insulator transition involves a discontinuous change in the molar volume [1–4]. Such a first-order transition can lead to phase coexistence of metallic and insulating states, where the length scales of these states are determined by strain and stress. In $(\text{La, Sr})\text{MnO}_3$ and $(\text{La, Ca})\text{MnO}_3$ [5], such phase coexistence has been observed for low concentrations of the divalent cation as droplets, and it results from competition between the “potential” and “kinetic” energy of the valence electron system. In manganite systems, extremely diverse types of phase separation can develop, occurring on a variety of length scales that can range from micrometers down to a few nanometers. Interestingly, phase coexistence not associated with metal-insulator transitions has also been observed; it can also arise from competition between different charge and orbitally ordered or disordered phases [6,7]. The spin, charge, and orbital orderings found in the manganites are often associated with large displacements of the ions in the lattice or even with changes in the molar volume. Generally, the orbital and charge ordering take place at higher temperatures than the magnetic ordering [8]. In both cases, the coupling between the different phases is mediated through coupling with the lattice. In contrast, the coupling of orbital and spin order is mostly of electronic nature by the antisymmetrization requirement of the wave function. In LaMnO_3 [9], the orbital interactions between the e_g electrons are much stronger ($T_{\text{OO}} \sim 800$ K) than the magnetic interactions ($T_N \sim 150$ K). In contrast, the Jahn-Teller active t_{2g} electrons in the vanadates orbitally order at $T_{\text{OO}} \sim 200$ K or lower. Although the difference between the spin and orbital ordering temperatures in $R\text{VO}_3$ (R = rare earth or Y) is smaller than that in the manganites, relatively little interaction between the spin and orbitally ordered states is observed. The orbital order-

ing temperature is higher than the magnetic ordering with the exception of LaVO_3 . For the small ionic size R in $R\text{VO}_3$, complex behavior has been observed in which different types of orbital ordering occur [10,11]. Here a change in the orbital structure is accompanied by a change in spin order. This indicates a strong coupling between the two types of order as required by the antisymmetric nature of the electron wave function, including spin and orbit. Nevertheless, the orders originate at distinctly different temperatures. Here we report the orbital ordering of SmVO_3 , in which coexistence of orbital orderings of different symmetry is triggered by magnetic ordering of the vanadium spins. This coexistence of orbital orderings is not associated with metal-insulator transitions but is the result of magnetic exchange striction, which provides the coupling to the lattice.

Polycrystalline samples of SmVO_3 were prepared by chemical reduction of SmVO_4 at 1400 °C under a H_2/N_2 atmosphere. The SmVO_4 powders were prepared by solid state reaction, using predried Sm_2O_3 (99.9%) and a 10% excess of V_2O_5 (99.95%) to compensate the V volatility which led to a small V_2O_3 impurity in the SmVO_3 sample. High resolution x-ray powder diffraction experiments were carried out on beam line ID31 at the European Synchrotron Radiation Facility (ESRF) in Grenoble. Short scans were performed during cooling to 5 K, where a long scan was measured after temperature stabilization. Then short scans up to 254 K were measured, while heating to room temperature (RT). The powder diffraction patterns were analyzed by the Rietveld method [12] using the GSAS program [13] as implemented in the EXPGUI package [14]. The specific heat was measured between 3 and 300 K using a relaxation method in a commercial quantum design physical properties measurement system.

SmVO_3 has an orthorhombic perovskite structure at RT, as is common for all $R\text{VO}_3$ consisting of corner-sharing oxygen octahedra. The vanadium is located in the center of the octahedron, and the samarium is located between the octahedra. We could index the peaks belonging to the SmVO_3 phase with the orthorhombic $Pbnm$ space group.

From the refinement of the diffraction pattern, we observed that SmVO_3 stabilizes in an O-orthorhombic structure at room temperature [15] ($a < c/\sqrt{2} < b$) because of the buckling of the corner-shared octahedra [16]. SmVO_3 retains its orthorhombic structure down to $T_{\text{OO}} = 200$ K. Here the symmetry changes to monoclinic $P2_1/b11$ [17] as evidenced by the splitting and broadening of the diffraction lines. We identify this change in symmetry with the orbital ordering transition. This is confirmed by the specific heat measurement, as shown in Fig. 1, and is consistent with other reports [11]. The value of the monoclinic angle α increases slowly from 90.00° at 200 K to $90.019(4)^\circ$ at 129 K (Fig. 2). As the temperature further decreases, the value of α increases rapidly to a maximum of $90.131(1)^\circ$ below 50 K (Fig. 1). The onset of orbital ordering is accompanied by a change in the unit-cell volume (Fig. 2). This monoclinic phase persists from the T_{OO} down to the magnetic transition at T_N [Fig. 3(b)], which is observed by both specific heat and magnetization measurements (Fig. 1).

Below 115 K, we observe a coexistence of phases with monoclinic and orthorhombic symmetries, which remains down to our lowest measurement temperature of 5 K [Fig. 3(c)]. The proportion of orthorhombic phase increases from 15% at 115 K to 25% at 5 K. Similar ratios were observed upon both cooling and warming the sample. We note that the phase coexistence sets in continuously below 115 K, where both phases have the same molar volume. The V-O1, V-O2, and V-O3 distances, where O1 are the out-of-plane and O2 and O3 are the in-plane oxygens, are important indicators of the type of orbital ordering of a system. In our data, they are difficult to determine accurately because Sm, a heavy rare earth, dominates the diffraction pattern and also because there is considerable overlap of peaks from the coexisting phases at low temperatures. However, as shown in Table I, the V-O distances confirm that the RT structure is not orbitally ordered and strongly suggest that at 5 K both the monoclinic and orthorhombic phases are orbitally ordered. The V-O distances [18] in the monoclinic and orthorhombic phases are comparable within error bars to those in the so-called *G*-type and *C*-type orbitally ordered phases of YVO_3 , respectively [19]. To confirm the nature of these phases over the whole temperature range, since the rapidly collected cooling/heating data do not allow a precise deter-

mination of the oxygen fractional coordinates [20], we have chosen the lattice parameter ratio b/a (Fig. 4) as an indicator of the type of orbital ordering and compared it to the ratios for other $R\text{VO}_3$ [21]. This comparison provides further evidence that the low-temperature orthorhombic phase of SmVO_3 is also orbitally ordered. For YVO_3 [19], HoVO_3 , and YbVO_3 , the transition from *G*- to *C*-type orbital ordering is discontinuous first-order, and a large drop of the b/a ratio can be observed. Moreover, it occurs at much lower temperature than the magnetic ordering. In contrast, for SmVO_3 the transition is continuous and is observed to set in very close to T_N .

The type of orbital ordering (OO) present in the ground state of the $R\text{VO}_3$ compounds depends mainly on the degree of octahedral tilting caused by the deviation in size of the rare-earth cation from that in the ideal cubic perovskite. Although all $R\text{VO}_3$ compounds initially order in the so-called *G*-type structure ($d_{xy}d_{yz}$ and $d_{xy}d_{xz}$ orbitals are occupied alternately along all three directions of the lattice), on increasing the octahedral tilting as the rare-earth cation becomes smaller, a first-order transition to a *C*-type OO ground state ($d_{xy}d_{yz}$ and $d_{xy}d_{xz}$ orbitals are occupied alternately in the ab plane while the same orbitals are occupied along c) occurs in the range 50–80 K for rare earths smaller than Tb [11]. This phase transition involves a large decrease in unit-cell volume. In these strongly distorted structures, the *C*-type ground state is largely stabilized by a shift of the *R* cation in order to maximize the *R*-O covalency [10,22]. SmVO_3 lies far into the *G*-type OO region of the phase diagram. As observed in our diffraction measurements, both the appearance of the *C*-type phase and the rapid increase in the monoclinic distortion of the *G*-type phase below 115 K (Fig. 2) are most likely associated with the onset of magnetic ordering.

It has long been known that magnetic exchange striction can occur at or shortly below T_N in transition metal oxides in order to increase the magnetic exchange interaction energy [23]. This has previously been observed in LaVO_3 [24,25] and CeVO_3 [24]. In the case of CeVO_3 , the type of OO remains the same, but the exchange striction occurring at T_N involves an overall decrease in the unit-cell volume. In the case of LaVO_3 , *G*-type OO arises 2 K below the magnetic ordering temperature and may itself be the result of exchange striction. However, in the

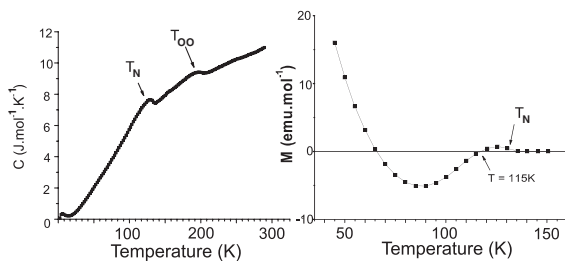


FIG. 1. Specific heat of SmVO_3 (left) and magnetization (in 1 kOe) (right).

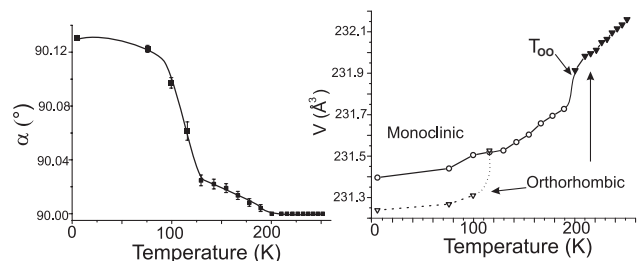


FIG. 2. Temperature dependence of alpha angle (left) and unit-cell volume (right) in SmVO_3 .

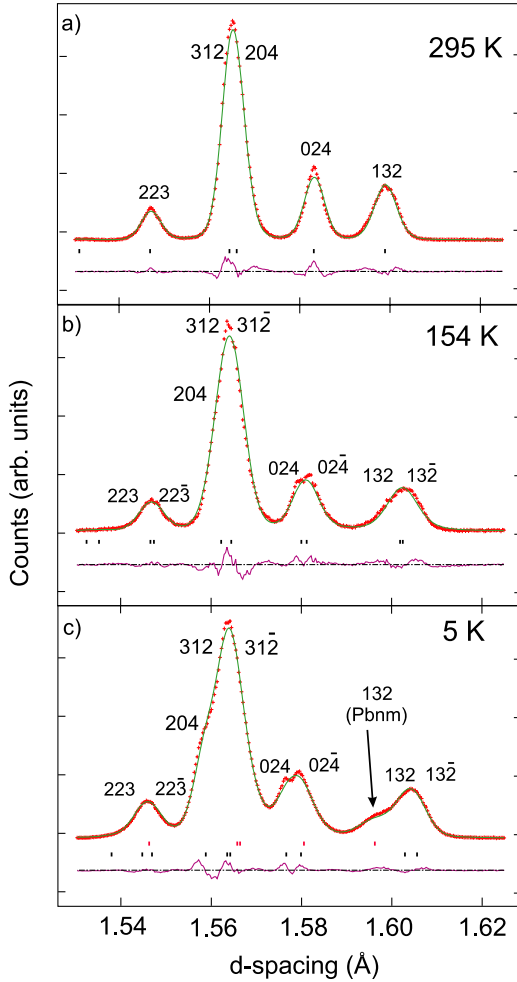


FIG. 3 (color online). Section of the diffraction pattern that shows the successive phases observed for SmVO_3 with (a) $T > T_{00}$: $Pbnm$ ($R_{wp} = 0.078$), (b) $T_N < T < T_{00}$: $P2_1/b11$ phase, (c) $T < T_N$: $Pbnm$ (top markers) and $P2_1/b11$ (bottom markers) phases ($R_{wp} = 0.0517$).

“small radius” $R\text{VO}_3$ compounds such as YVO_3 , the structural change at T_N is tiny [26]. The difference between the orbital and magnetic ordering temperatures in these compounds is much greater than in LaVO_3 and CeVO_3 [11], and the orbital ordering is fully developed at T_N [10]. Therefore, there is little further energy to be gained through a structural distortion.

TABLE I. V-O bond lengths (\AA) for SmVO_3 in the orbitally ordered phases at 5 K and nonordered phase at 295 K.

	5 K ($Pbnm$)	5 K ($P2_1/b11$)	295 K ($Pbnm$)
V1-O1	2.026(5)	1.996(15)	1.9942(12)
V1-O2	1.977(12)	1.973(16)	2.0236(35)
V1-O2	2.025(12)	2.070(14)	2.008(34)
V2-O1		1.934(15)	
V2-O3		2.024(13)	
V2-O3		2.049(16)	

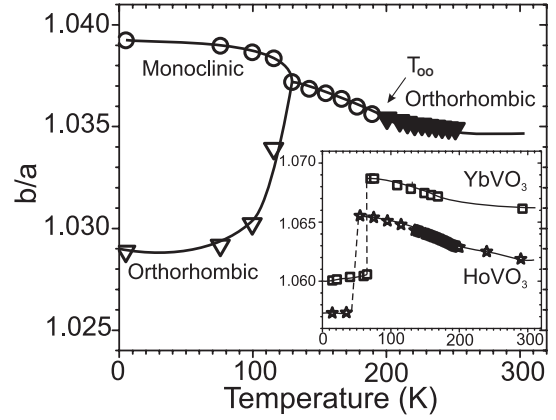


FIG. 4. Temperature dependence of the lattice parameter ratio b/a in SmVO_3 : The filled triangles represent the orthorhombic phase above T_{00} . The inset presents this ratio for other $R\text{VO}_3$ with $R = \text{Ho}$ (stars) and Yb (squares).

The exchange striction occurring at T_N in SmVO_3 is expected to be intermediate in magnitude between that in CeVO_3 and YVO_3 ; the value of α suggests that orbital ordering in the G -type phase is incomplete at this point (Fig. 1). Since the exchange striction appears to cause a volume decrease, one may expect the onset of magnetic ordering to promote the C -type phase; that is, it will be lowered in energy to an extent that depends on the magnitude of the exchange striction. For compounds such as CeVO_3 , the G -type phase is much lower in energy at all temperatures due to the smaller degree of octahedral tilting. At the other end of the phase diagram, the exchange striction in the G -type phase at T_N is too weak to have any effect on the crystal structure. However, for materials closer to the phase boundary such as SmVO_3 , the exchange striction is still significant and may be strong enough to lower the energy of the C -type phase enough to become favored.

Somewhat surprisingly, in SmVO_3 the unit-cell volumes of the two OO phases are equal (at the precision of our diffraction measurements) immediately below T_N (Fig. 2). However, this can be explained by a scenario where small droplets of the C -type phase are initially formed in a G -type matrix. Although the C -type droplets can be distinguished by x-ray diffraction, implying coherent OO over length scales of at least several hundred angstroms, they are still relatively small and isolated compared to the surrounding G -type phase. The unit-cell volume of regions of a droplet close to an interface will be forced to match that of the surrounding matrix, and large strain fields will thus extend throughout droplets that are small. On further cooling, the C -type droplets will tend to enlarge and coalesce into domains big enough for relaxation of the strain to take place. This relaxation is seen in the rapid decrease of the unit-cell volume as the fraction of the C -type phase grows. However, the remaining strain might still be large enough to inhibit further transformation of the G -type matrix, stabilizing the phase-separated state with little

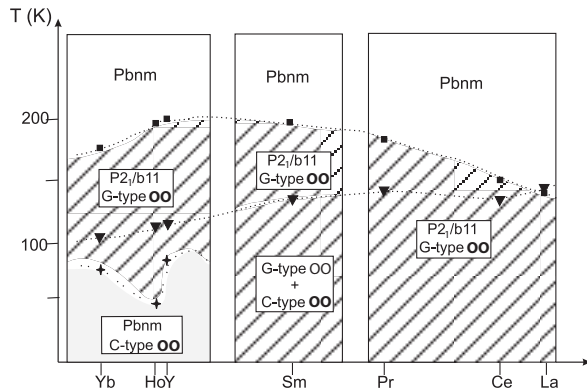


FIG. 5. Phase diagram obtained for RVO_3 studied by diffraction techniques. Squares represent the onset of orbital ordering; triangles represent spin ordering; stars represent the first-order transition.

change in phase fractions below 80 K. The difference in unit-cell volumes of the two phases at 5 K is 0.067%, which can be compared to changes of 0.16% on cooling through the first-order transition in YVO_3 [19], 0.15% in $HoVO_3$, and 0.16% in $YbVO_3$ [21], where full transformation to the *C*-type phase is achieved. The suppressed volume decrease in $SmVO_3$ is further evidence that significant strain remains in the system down to 5 K.

Although specific heat measurements show no transition between orbital orderings below T_N in other “intermediate radius” vanadates such as $EuVO_3$, $GdVO_3$, and $TbVO_3$ [11], the low-temperature phase composition of these materials has thus far not been studied by techniques such as high resolution x-ray diffraction. It remains to be seen whether these materials will also display phase separation between the two types of OO. On one hand, the tendency towards *C*-type OO increases with smaller rare-earth radius, but, on the other hand, the exchange striction at T_N that appears to promote transformation to the *C*-type phase is expected to decrease in magnitude. Nevertheless, it is likely that the border between the *C*- and *G*-type phases as a function of ionic radius is not a sharply defined line, as suggested by the phase diagram of Miyasaka *et al.* [11] but rather occurs via a broad phase-separated region. We thus use diffraction data to propose a modified RVO_3 phase diagram in Fig. 5. In summary, high resolution x-ray diffraction has demonstrated that vanadium spin ordering in $SmVO_3$ induces magnetic exchange striction that changes the symmetry of the orbital ordering in part of the sample. The two types of orbital ordering then coexist down to low temperature, a situation that is stabilized purely by lattice strains associated with the difference in unit-cell volumes of the two phases.

We thank Dr. I. Margiolaki for experimental assistance at ESRF and for useful discussions on the x-ray diffraction experiments. We are grateful to Professor D.I. Khomskii for enlightening and stimulating discussions. We acknowledge financial support by the European project SCOOTMO RTN (Contract No. HPRN-CT-2002-00293).

*Corresponding author.

Electronic address: t.t.m.palstra@rug.nl

- [1] Y. Tokura and Y. Tomioka, *J. Magn. Magn. Mater.* **200**, 1 (1999).
- [2] E. Dagotto, T. Hotta, and A. Moreo, *Phys. Rep.* **344**, 1 (2001).
- [3] E.L. Nagaev, *Colossal Magnetoresistance and Phase Separation in Magnetic Semi-conductors* (Imperial College Press, London, 2002).
- [4] C. Sen, G. Alvarez, and E. Dagotto, *Phys. Rev. B* **70**, 064428 (2004).
- [5] J.C. Loudon, N.D. Mathur, and P.A. Midgley, *Nature (London)* **420**, 797 (2002).
- [6] P.G. Radaelli *et al.*, *Phys. Rev. B* **63**, 172419 (2001).
- [7] J.P. Chapman *et al.*, *Dalton Trans.* **19**, 3026 (2004).
- [8] Y. Murakami *et al.*, *Jpn. J. Appl. Phys.* **38**, Suppl. 1, 360 (1999).
- [9] Y. Murakami *et al.*, *Phys. Rev. Lett.* **81**, 582 (1998).
- [10] G.R. Blake *et al.*, *Phys. Rev. Lett.* **87**, 245501 (2001).
- [11] S. Miyasaka, Y. Okimoto, M. Iwama, and Y. Tokura, *Phys. Rev. B* **68**, 100406 (2003).
- [12] H.M. Rietveld, *J. Appl. Crystallogr.* **2**, 65 (1969).
- [13] A.C. Larson and R.B. von Dreele, Los Alamos Laboratory Report No. LAUR 86-748, 1994.
- [14] B.H. Toby, *J. Appl. Crystallogr.* **34**, 210 (2001).
- [15] J.B. Goodenough and J.M. Longo, in *Crystallographic and Magnetic Properties of Perovskite and Perovskite-Related Compounds*, edited by K.-H. Hellwege, Landolt-Bornstein, New Series, Group III, Vol. 4a (Springer-Verlag, Berlin, 1970), Chap. 3, p. 126.
- [16] A.M. Glazer, *Acta Crystallogr. A* **31**, 756 (1975).
- [17] We use $P2_1/b11$ for the monoclinic phase instead of the standard $P2_1/c$ to allow a direct comparison of the lattice parameters, Miller indices, and atomic coordinates with those of the orthorhombic *Pbnm* phases.
- [18] See EPAPS Document No. E-PRLTAO-96-087604 for a full list of refined atomic parameters, bond lengths, and angles. This document can be reached via a direct link in the online article’s HTML reference section or via the EPAPS homepage (<http://www.aip.org/pubservs/epaps.html>).
- [19] G.R. Blake *et al.*, *Phys. Rev. B* **65**, 174112 (2002).
- [20] These data sets were collected over 5–10 minutes and, although sufficient for a precise determination of the lattice parameters, cell volume, monoclinic angle, and phase fractions, below T_{OO} the accurate determination of oxygen fractional coordinates was not possible; the atomic parameters were thus fixed to those determined for the $P2_1/b11$ and *Pbnm* phases at 5 K.
- [21] G. Blake *et al.* (to be published).
- [22] T. Mizokawa, D.I. Khomskii, and G.A. Sawatzky, *Phys. Rev. B* **60**, 7309 (1999).
- [23] S. Greenwald and J.S. Smart, *Nature (London)* **166**, 523 (1950).
- [24] Y. Ren *et al.*, *Phys. Rev. B* **67**, 014107 (2003).
- [25] P. Bordet *et al.*, *J. Solid State Chem.* **106**, 253 (1993).
- [26] C. Marquina *et al.*, *J. Magn. Magn. Mater.* **290–291**, 428 (2005).